Biosensors and Bioelectronics 129 (2019) 182–188

Contents lists available at ScienceDirect

Biosensors and Bioelectronics

journal homepage: www.elsevier.com/locate/bios

A sensitive electrochemical genosensor for highly specific detection of thalassemia gene

Mohammad-Bagher Gholivand*, Arezoo Akbari

Department of Analytical Chemistry, Razi University, Kermanshah, Iran

ARTICLE INFO

Keywords:
β-Thalassemia
Aminothiophenol
Graphene oxide
Electrochemical biosensor

ABSTRACT

Beta thalassemias (βth) are the result of mutations in the β-globin gene. In this report, an electrochemical genosensor was made to detect the sequences anent with the β-globin gene. This biosensor is based on immobilizing 20-mer single stranded oligonucleotide (probe) on the Au nanoparticles- poly (4-aminothiophenol)/ reduced graphene oxide/glassy carbon electrode (AuNPs-PAT/rGO/ GCE) and hybridizing this oligonucleotide along with its complementary sequence (target). The vastness of the probe and target sequences hybridization was studied through differential pulse voltammetry (DPV) along with electrochemical impedance spectroscopy (EIS) using the $[Fe(CN)6]^{3-}/^{4-}$ (1:1) as a hybridization index. The biosensor indicated great efficiency with significant sensitivity along with favorable selectivity. The DPV and EIS responses with the intended concentrations of the sequence were linear varying from 1.0 pM to 400.0 pM (I_p ν log C) and 0.5–400.0 pM (ΔR_{ct} ν log C) with a limit of detection of 0.06 pM and 0.035 pM, at the signal to noise ratio of 3σ. The biosensor of the DNA indicated proper discrimination capability to mismatched two-base, three-base, and non-complementary sequences.

1. Introduction

The growing demand for rapid, simple, inexpensive and portable testing methods instead of the expensive and time-consuming methods for specific sequences detection in nucleic acids has encouraged research in the field of DNA sensors or genosensors. DNA sequence polymerization (PCR) and DNA hybridization (FISH) are commonly used methods for specific sequences detection in nucleic acids that not only have the above-mentioned drawbacks but also are laborious. A variety of DNA sensors as the most attractive alternative have been proposed for the detection of DNA sequences including optical (Scarano et al., 2010), piezoelectric (Lucarelli et al., 2008) and electrochemical (Sadik et al., 2009) transduction. Electrochemical gene sensors show attractive features such as high sensitivity, fast response and cost-effectiveness needed for the preliminary detection of diseases, preventative therapy of genetic disorders, and the treatment of bacterial and viral infections (Kashish et al., 2015). Electrochemical DNA genosensors consist of a DNA probe immobilized onto the electrode surface. This probe is bound to a specific target DNA sequence, generating an electrical signal (Dolatabadi et al., 2011).

Signal amplification in DNA based sensors is usually achieved through various surface modifications. Advancements in nanomaterials science offer amazing opportunities for making new, sensitive biosensors. Nanomaterial based platforms find wide use in many electrochemical, electroanalytical and bioelectrochemical applications. Nanoscale materials such as metal nanoparticles (Zare and Shabani, 2016; Oliveira et al., 2018; Sharma et al., 2018), metal oxides (Low et al., 2017; Jiang et al., 2018), carbon allotropes (Frias et al., 2017; Jaiswal et al., 2018; Mohammadian and Faridbod, 2018) and conductive polymers (Wang et al., 2015; da Silva et al., 2017; Moon et al., 2018) offer some outstanding prospects for designing new bioelectronic devices exhibiting novel functions. Due to excellent properties such as conductivity, simple synthesis, good aqueous dispersibility, large surface area, and good biocompatibility, graphene oxide (GO) and reduced graphene oxide (rGO) have found applicability in the field of biosensing (Lu et al., 2009; Chen et al., 2012) rGO alone or its composite with other materials (Zhou et al., 2009; Chen et al., 2011; Cai et al., 2014; Shamsipur et al., 2016). Reports indicate that the presence rGO has increased the surface area and speed of electron transfer process. AuNPs offer great nanoplatforms to interact with biological systems and thus have been applied in genosensor construction (Shi et al., 2014; Tiwari et al., 2015; Zhao et al., 2015). The incorporation of AuNPs into rGO increases the surface area, and adsorption of immobilized ssDNA probe molecules results in amplified signals in analyte detection. To increase the uniformity of the dispersed metal particles at the electrode surface, a conducting polymer with entrapping ability of metal nanoparticles

* Corresponding author.
E-mail address: mbgholivand@ac.ir (M.-B. Gholivand).

https://doi.org/10.1016/j.bios.2019.01.017
Received 12 October 2018; Received in revised form 3 January 2019; Accepted 4 January 2019
Available online 15 January 2019
0956-5663/

into its matrix has been advised (Shin and Huh, 2012; Wilson et al., 2012). 4-Aminothiophenol (AT) as one of this class compound with nanoparticles assembling ability via covalent or electrostatic interactions, has attracted significant attention. The presence of thiol group in AT structure assembled the AuNPs and resulted in unique morphology.

Thalassemia is a genetic blood disorder passed down through families (inherited). Due to a disease-causing variant in one or more of the globin genes, a disruption in the normal ratio of alpha globin to beta globin production is created and results in a microcytic anemia of varying degree. There are two primary types of Thalassemia disease: Alpha Thalassemia disease and Beta Thalassemia disease. Beta Thalassemia Major (also called Cooley's Anemia) is a serious illness. Its symptoms appear in the first two years of life and include paleness of the skin, poor appetite, irritability, and failure to grow. The increasing interest in biosensors and especially genosensors during recent years, and reporting only one genosensor for Thalassemia detection (Hamidi-Asl et al., 2016) encourage us to fabricate a simple, portable equipment with lower costs, compared to the more classical techniques.

In the present study a DNA biosensor based on one-step electroploymerization of 4-aminothiophenol monomer and Au nanoparticles on reduced graphene oxide /Glassy carbon electrode (rGO /GCE) that was utilized as a tool for sensing ultra-traces of β-globin gene. Au nanoparticles were electrochemically disturbed into the matrix of conductive polymer, assembled on the surface of rGO /GCE electrode. The thiolated strand of human β-thalassemia gene was attached to AuNPs covalently through a self-assembly approach as the probe to detect β-globin gene (antisense strand of human β-thalassemia gene).

2. Experimental

2.1. Reagents and materials

A 20-mer oligonucleotide related to human β-thalassemia gene sense-strand (IVSII-1)) and its complementary (CIVSII-1) oligonucleotide related to antisense strand of human β-thalassemia gene were utilized as probe and target DNA. DNA oligonucleotides along with the sequences that follow were achieved from Fazabiotech Co. (Tehran, Iran):

Probe DNA (pDNA): 5′-SH-ACTTCAGGATGAGTCTATGG-3′ (IVSII-1)
Complementary DNA (cDNA): 5′-CCATAGACTCATCCTGAAGT-3′ (CIVSII-1)
Non-complementary sequences (ncS): 5′-AATCTCATGGCCGATTC GTT-3′
Double-base mismatched DNA (dbmDNA): 5′-CGATTGACTCATCCT GAAGT-3′
Three-base mismatched DNA (tbmDNA): 5′-CGATTGACACATCCTG AAGT-3′

All stock solution of oligonucleotides (100 μM) was made ready using deionized water and was kept frozen.

All chemicals had the analytical grade and were utilized as received. Graphene oxide, sodium phosphate dibasic, bovine serum albumin (BSA), 4-aminothiophenol (AT), sodium tetrachloroaurate (III) dihydrate ($NaAuCl_4{\cdot}3H_2O$), potassium hexacyanoferrate (II) trihydrate ($K_4Fe(CN)_6{\cdot}3H_2O$), H_2SO_4, potassium hexacyanoferrate(III) ($K_3Fe(CN)_6$),sodium phosphate monobasic, and $HClO_4$ were gained from Sigma-Aldrich (Madrid, Spain). All the specimens were developed in 0.1 M phosphate buffer (PBS, pH = 7.4) and kept at 4 °C prior to application. Ultrapure water was gained from a system of Mill-Q water purification.

2.2. Apparatus

Electrochemical tests were done with the help of an Autolab (Eco Chemie BV, Netherlands) being controlled using NOVA software1.8. A common cell was utilized along with saturated calomel electrode (SCE), Pt wire and modified electrode as reference, counter and working electrodes. The solutions pH was adjusted by a JENWAY-3510 pH meter equipped with a combined glass electrode. The scanning electron microscopy (SEM) (Philips XL 30) was used for morphology study.

2.3. Producing modified electrode

Alumina (1.0 and 0.05 μm) was used to polish bare GCE and then was completely cleaned and made free adsorbed particle by distilled water washing and ethanol container bath ultrasonicating for 10 minutes. 5 μL of 1 mg mL^{-1} aqueous solution GO was dropped on the GCE surface. After drying, GO film was reduced electrochemically in a N_2-saturated phosphate buffer (0.1 M, pH 7.4) by cyclic voltammetry (CV) at potential window of −1.5–0.0 V using scan rate of 100 mV s^{-1} throughout 40 cycles. The rGO/ GC electrode was washed using water and submerged in a solution 0.2 mM $NaAuCl_4$, 0.5 M H_2SO_4 and 10 mM AT. CV technique was applied for electrochemical deposition using a repetitive potential scan between −0.5 - + 1.7 V (versus SCE) at a scan rate of 50 mV s^{-1} for 50 cycles (Fig. S1). Poly (4-aminothiophenol) (PAT) film containing Au nanoparticles were made on the surface of rGO/ GC electrode simultaneously.

2.4. Working electrode activation

The working electrode surface was activated by cyclic voltammetry in 0.50 M $HClO_4$ without stirring at the potential range 0.0–0.8 V and scan rate of 100 mV s^{-1} for 20 cycles.

2.5. Immobilizing the probe on the working electrode

The immobilizing the pDNA on the activated AuNPs-PAT/rGO/ GCE was carried out by dropping of 5 μL of 0.1 μM pDNA solution on its surface and incubating for 2 h at ambient temperature. pDNA along the thiol groups at 5-end were covalently bonded to the AuNPs presented in the modified electrode body through Au–S binding. To remove unspecific adsorbed DNA probe, the pDNA/AuNPs-PAT/rGO/ GC electrode was washed using deionized water. Ultimately, to block the free sites and reduce the non-specific bindings, the electrode was submerged into the BSA solution (0.25%) for 15 min.

2.6. Hybridization

The hybridizing process was done by casting 10 μL cDNA with different concentrations on the pDNA/Au NPs-PAT/rGO/ GCE surface, and keeping it for 35 min at the ambient temperature, and then to remove the non-specifically adsorbed DNA, the hybridized electrode was rinsed using PBS (pH 7.4).

2.7. Electrochemical detection

The sensing ability of the pDNA/AuNPs-PAT/rGO/ GC electrode toward cDNA was evaluated by EIS and differential pulse voltammetric (DPV) techniques based on “signal on” and “signal off” strategies, respectively. In the impedimetric determination, after hybridization of 10 μL of the cDNA with different concentrations at the pDNA/AuNPs-PAT/rGO/ GCE surface and incubation for 35 min, the electrode was washed using phosphate buffer and was utilized for recording of the EIS responses of 0.1 M phosphate buffer solution (PBS, pH 7.4) containing 5.0 mM of $[Fe(CN)_6]^{3-/4-}$ couple (1:1) as external probe. The obtained results showed that the charge transfer resistance (R_{ct}) is raised by increasing the accumulated cDNA at the electrode surface showing s a “signal on” strategy signifying that the hybridization is occurring at the genosensor surface. The difference between responses of the pDNA/AuNPs-PAT/rGO/ GCE before and after hybridization with cDNA ($\Delta R_{ct} = R_{ct}(cDNA)-R_{ct}(pDNA)$) was used as the measurement signal.

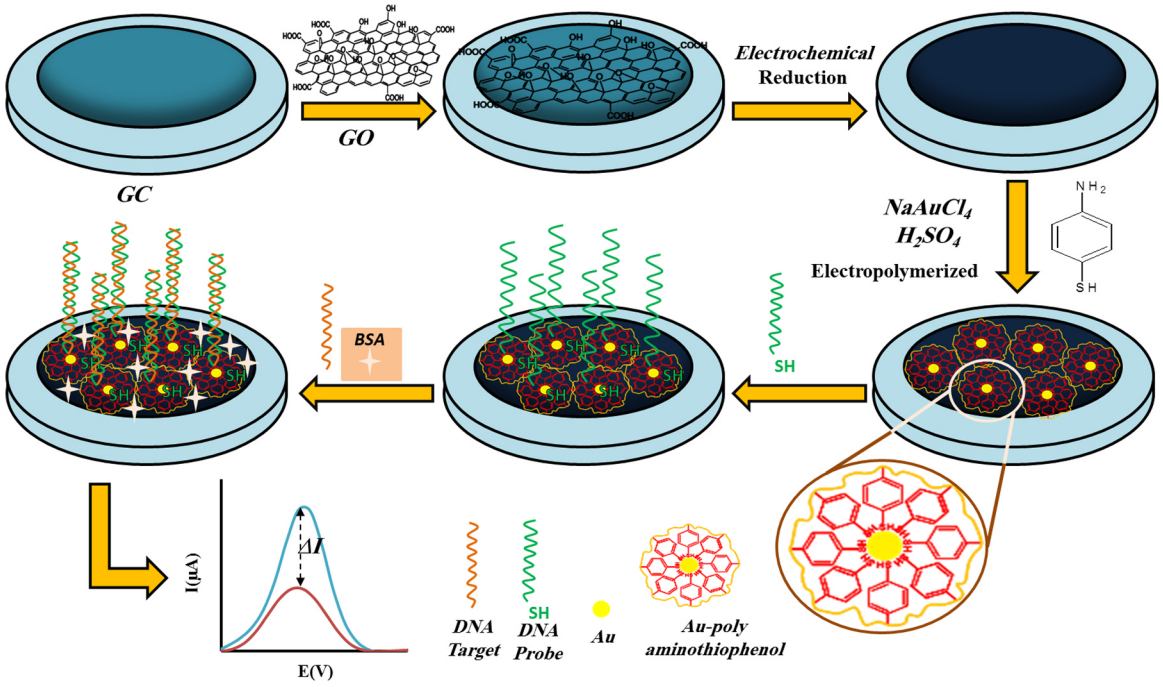

Scheme 1. Fabrication and detection process of the DNA biosensor.

Moreover, the DPV was utilized instead of the above sensing strategy. Throughout these experiments, $[Fe(CN)6]^{3-/4-}$ was used as a cheap external probe with proper electrochemical behavior. To design the "signal off" determination by DPV approach, 10.0 μL of cDNA with different concentration was dropped on to the surface of the pDNA modified electrode and incubated for 35 min. The washed electrode was immersed in 0.1 M PBS (pH = 7.4) containing 5.0 mM of $[Fe(CN)6]^{3-/4-}$ couple (1:1) and its DP voltammogram under pulse amplitude of 50 mV and potential window of 0.0–0.4 V was recorded. The reduction in peak current (I_p) was dependent on the cDNA concentration.

Regeneration of the biosensor was carried out in NaOH solution (0.1 M for 10 min at room temperature) by regeneration and rehybridization cycles (Fig. S2a and S2b).

The DNA biosensor fabrication and detection processes were schematically shown in Scheme 1.

3. Results and discussion

3.1. Field emission gun scanning electron microscope (FE-SEM) study

To study the surface morphology, the outcome SEM image of the modified electrodes (Fig. 1) was utilized.

As it is clear from Fig. 1A, SEM image of rGO indicted a planar sheet-like structure, showing that rGO had been readily exfoliated into separate sheets on the surface of electrode. When AT was electro polymerized on rGO surface (Fig. 1B), as expected, polymeric film PAT was shaped on the surface. rGO modifications by PAT and AuNPs are seen in Fig. 1C. As shown, the Au nanoparticles are distributed uniformly as -SH functional groups shown in PAT assist to anchor the Au nanoparticles.

EIS as a suitable and sensitive tool was utilized to study the electron transfer process occurring at electrodes-solution interface. The diameter of the semicircle segment of impedance spectra at high frequencies, correspond to the electron transfer resistance, (R_{ct}) and its linear part at lower frequencies, depicts the diffusion-limiting step of the electrochemical process. The typical Nyquist plots of bare GC bare(a), rGO/GC (b), AuNPs-PAT/rGO/GC(c), pDNA/AuNPs-PAT/rGO/GC (d) and BSA/pDNA/AuNPs-PAT/rGO/GC (e) electrodes which have been recorded at frequencies ranging from 0.01 Hz to 10 kHz, and formal potential of 0.189 V in 0.1 M PBS (pH 7.4) accompanied with 5 mM $[Fe(CN)_6]^{3-/4-}$ as an electrochemical redox probe are shown in Fig. 2. Randles equivalent circuit (Fig. 2A, inset) was used during modifications. The bare GCE (curve a) showed a tiny semicircle whose charge transfer resistance was 436 Ω. After modifying the GCE by rGO, EIS spectrum showed a straight line indicating the role of rGO in facilitating the transfer of electron at the electrode surface (curve b). Further modification of rGO/GCE with AuNPs-PAT, increased the charge transfer resistance relative to rGO/GCE (curve c), which might be because of worse conductivity of the polymer film. After immobilizing the pDNA at the AuNPs-PAT/rGO/GC electrode surface, there was an increase in the R_{ct} value (193 Ω) which could be ascribed to the repellence of redox probe from approaching electrode surface by negative-charged phosphate skeletons of DNA (curve d). Finally after blocking the free sites of pDNA/AuNPs-PAT/rGO/GCE by immersing it in BSA solution the R_{ct} of the resulted electrode was further increased (246 Ω, curve e) which is due to reduction in effective surface area. Similar outcomes were also achieved using cyclic voltammetry (Fig. 2B).

The IR spectra of GO, rGO, AuNPs-PAT/rGO and pDNA/AuNPs-PAT/rGO were recorded and the results have been reported in supplementary file (Fig. S3).

3.2. Genosensor parameters optimization

In the study, to evaluate the effect of parameters such as target incubation time and pDNA concentration on the genosensor response, DPV method was utilized. The decline in the peak current of the probe modified electrode before and after cDNA hybridization (ΔI) was used as the response signal.

Moreover, the target incubation time is a vital effective factor in the genosensor response (Liu et al., 2010; Shamsipur et al., 2016). Therefore, the effect of incubation time of cDNA (20.0 pM) on the sensor response was examined with the findings, which is indicated in Fig. 3A. As seen, the current response boosted drastically with an increase in incubation time up to 35 min and leveled off after 35 min, which shows that the hybridization reaction was mostly finished after 35 min. We chose 35 min as the best DNA hybridization time.

To sidestep the non-specific adsorption of the cDNA, and providing false positive signal, optimization of the pDNA concentration on the

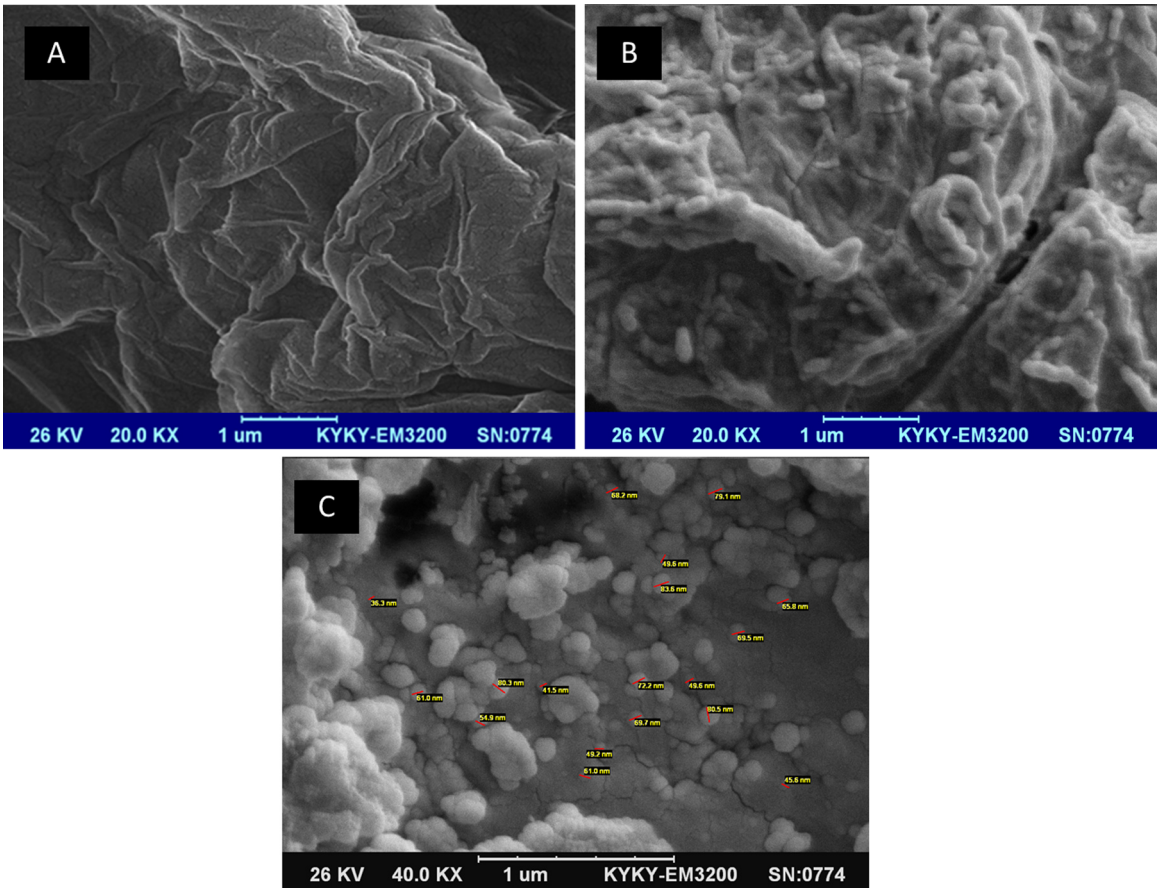

Fig. 1. SEM images of rGO/GCE (A), PAT/rGO/GCE (B), and AuNPs -PAT/rGO/GCE (C).

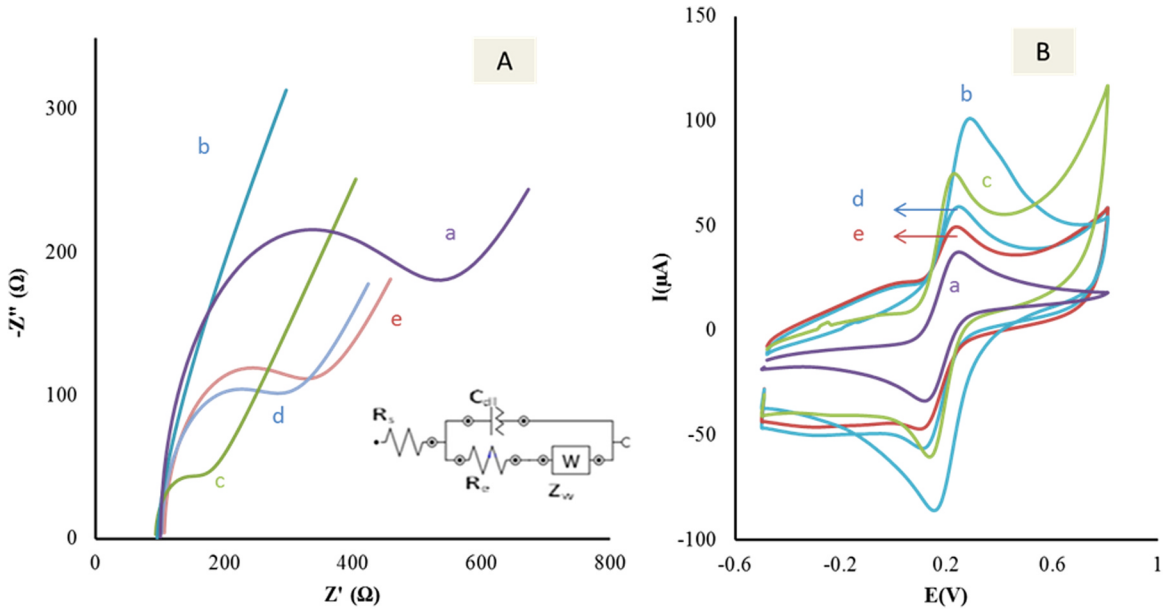

Fig. 2. A) Impedance spectra (Nyquist plots) and B) CVs of bare GC (a), rGO/GC (b), AuNPs-PAT/rGO/GC(c), pDNA/AuNPs-PAT/rGO/GC (d) and BSA/ pDNA/ AuNPs-PAT/rGO/GC (e) recorded in the solution of 0.1 M phosphate buffer of pH 7.4 containing 5.0 mM of $[Fe(CN)_6]^{3-/4-}$ couple (1:1).

performance of genosensor was carried out. The probe density was controlled by changing the concentrating pDNA in the range of 5 nM to 0.3 μM, and its effect on the genosensor response was examined and the outcomes were summarized in Fig. 3B. As it is clear, the maximum immobilization and hence the best response (ΔI) was achieved at the pDNA concentration of 0.1 μM and thus this amount of pDNA was used

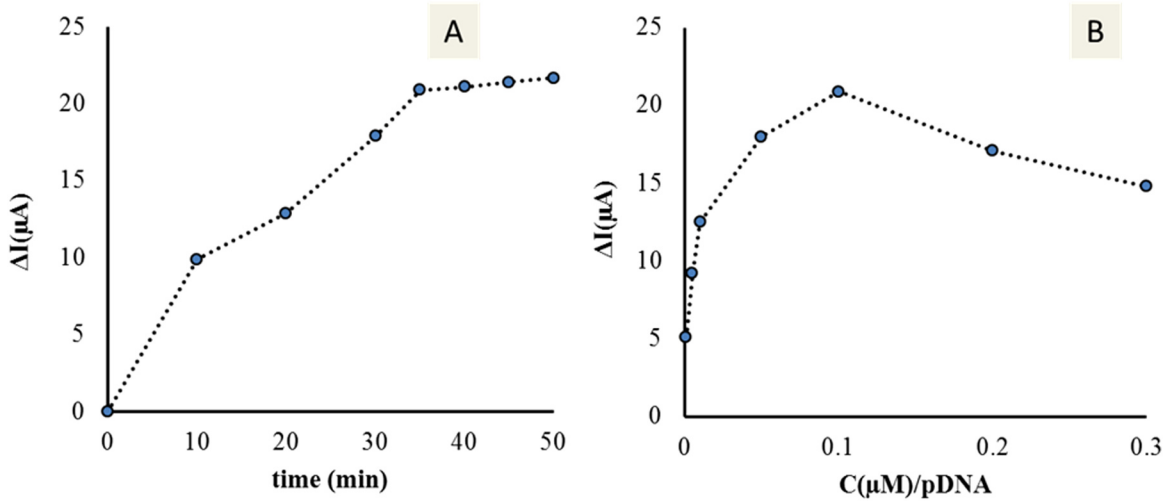

Fig. 3. Effect of incubation time of cDNA (20 pM) (A) and pDNA concentration (B) on DPV responses of the solution of 0.1 M phosphate buffer(pH 7.4) of containing 5.0 mM of $[Fe(CN)_6]^{3-/4-}$.

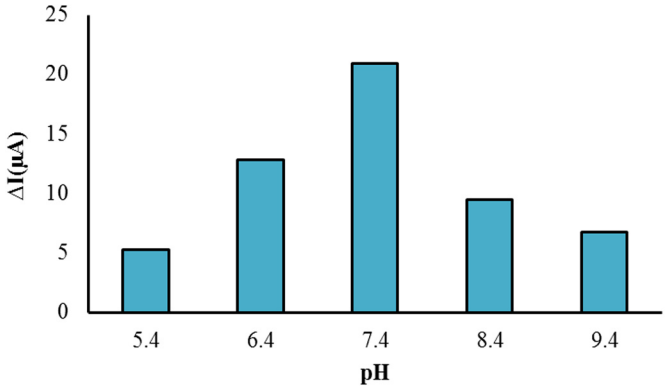

Fig. 4. Effect of pH of solution on the response of genosensor to 20.0 pM cDNA on DPV responses the solution of 0.1 M phosphate buffer of containing 5.0 mM of $[Fe(CN)_6]^{3-/4-}$.

throughout the experiment.

The influence of pH as the other parameter on the performance of the prepared genosensor was also studied. Fig. 4 indicates the effect of pH ranging from 5.4 to 9.4 on the genosensor signal to 20.0 pM of cDNA. The maximum sensitivity was achieved at pH 7.4 (Fig. 4). Thus, pH 7.4 was selected as the optimum pH for further uses.

3.3. Analytical performance of genosensor

Under optimal conditions, the sensitivity of the pDNA/AuNPs-PAT/rGO/GCE DPV toward the various concentration of cDNA was evaluated using DPV and EIS. In this investigation, 0.1 M PBS with pH = 7.4 as supporting electrolyte and 5.0 mM of $[Fe(CN)_6]^{3-/4-}$ as external redox probe were used. Fig. 5a reveals the DP voltammograms s of the foregoing sensor to cDNA with different concentrations. As it was expected, the peak current was linearly reduced by increasing cDNA concentrations that vividly indicates a "signal off" process. Incubation of cDNA at pDNA/AuNPs-PAT/rGO/GC electrode surface increases the number of [pDNA]-[cDNA] conjugates and prevents the diffusion of the external probe toward to electrode surface whose results are reducing in peak current. The ΔI was linear with the logarithm of the cDNA concentrating in the range from 1.0 pM to 400.0 pM and followed up from the regression equation of I (μA) = -8 $\log C_{[cDNA]/(pM)}$ + 30.0 (R^2 = 0.9974) (Fig. 5b). The limit of detection (LOD) of the proposed "signal off" genosensor for the analysis of the concentrating target DNA was 0.06 pM, at the S/N ratio 3σ, in which σ is the relative standard deviating a blank solution (n = 10).

To monitor the target DNA according to a "signal on" response, the EIS approach was also utilized. The pDNA modified electrode loaded with various concentration of cDNA after 35 min of incubation was submerged in foregoing supporting electrolyte containing $Fe(CN)_6]^{3-/4-}$ and the variation in the R_{ct} value was tracked. R_{ct} values changed with the variety in cDNA amounts (Fig. 5c). This implies the hybridization is happening at the genosensor because more negatively charged phosphate backbones are collected. Subsequently, the R_{ct} value expands following the development of double stranded DNA. The different between the R_{ct} of the pDNA/AuNPs-PAT/rGO/GCE before and after hybridization with cDNA (ΔR_{ct} = R_{ct}(cDNA)- R_{ct}(pDNA)) was utilized as the measurement signal. The linearity between the analytical signal (ΔR_{ct}) with the logarithmic value cDNA ranging from 0.5 to 400 pM follows the following equation (Fig. 5d):

$$\Delta R \ (\text{Ohm}) = 1316.1 \ \log C_{[cDNA]/(pM)} + 582.56 \quad (R^2 = 0.9976)$$

The calculated detection limit (S/N = 3σ, n = 10) was 0.035 pM.

The results showed that the proposed sensor is able to detect the cDNA with a wide linear range and a very low LOD successfully.

3.4. Stability, reproducibility, repeatability and selectivity study

To examine the genosensor stability, it was submerged in phosphate buffer of pH 7.4 for about 10 days and kept in fridge at 4 °C, after which the peak current reduced only to 5.2% of its initial current, which shows an acceptable stability. When the modified electrode was kept at the room temperature (34 °C) for 15 days under the identical conditions, just 14.6% of the peak current reduced. The good stability could be because the DNA sequences were tightly attached to the surface of pDNA modified electrode.

The genosensor reproducibility was evaluated utilizing five individual genosensors prepared under similar conditions for monitoring of 20.0 pM of cDNA. The outcomes showed a relative standard deviation (RSD) of 3.8% for DPV signals indicated. The outcome of the five replicate determinations of cDNA solution (20 pM) using one electrode under the optimal conditions ended in an RSD 2.1%. The obtained results show that the repeatability and reproducibility of the sensor are acceptable.

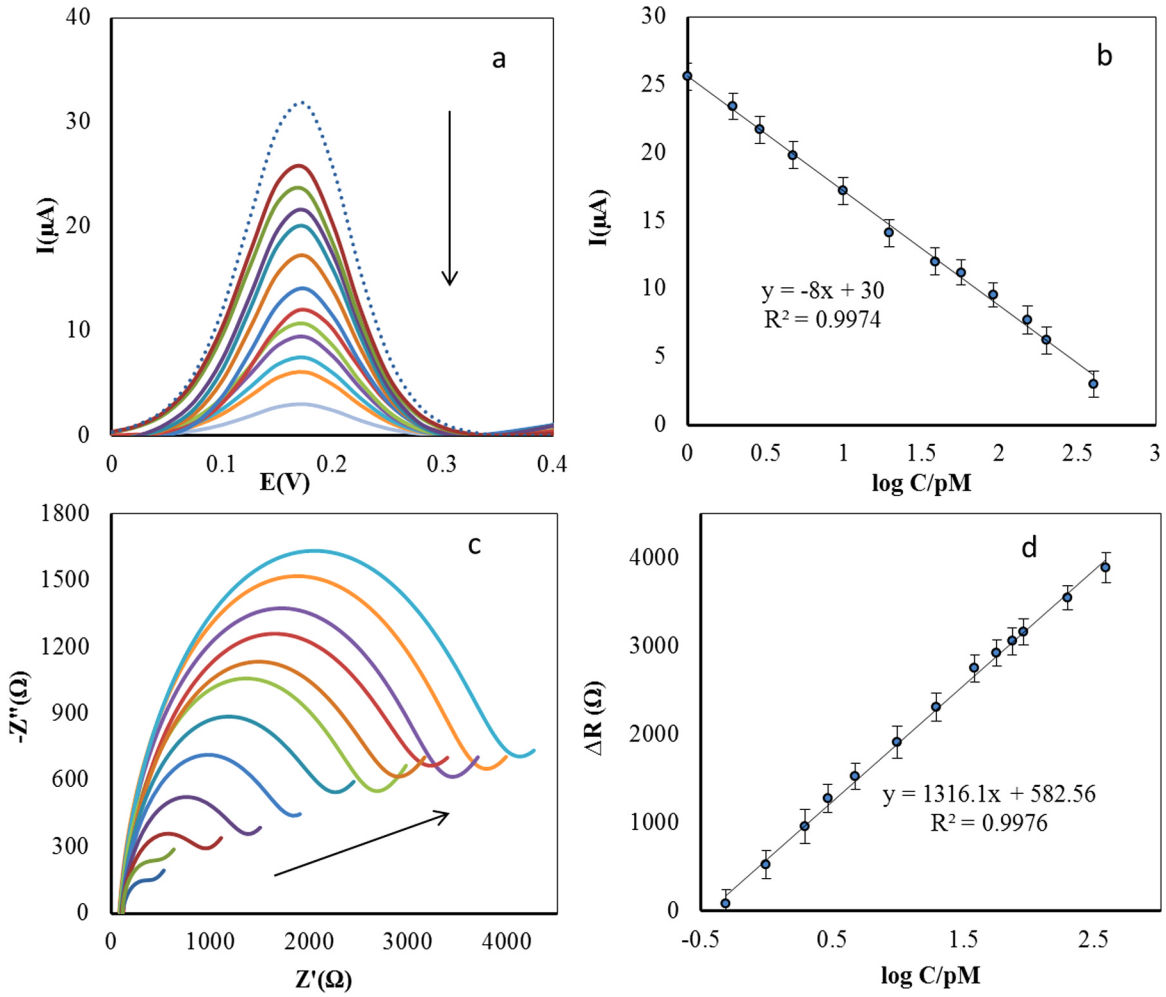

Fig. 5. (a) DPV responses of the pDNA/AuNPs-PAT/rGO/GCE recorded in 0.1 M phosphate buffer (pH 7.4) and 5.0 mM $[Fe(CN)_6]^{3-/4-}$, after incubation in the different concentrations of cDNA. (b) Calibration curve of DPV peak current versus logarithm of cDNA concentration. (c) Nyquist plots of the pDNA/AuNPs-PAT/rGO/GCE recorded in 0.1 M phosphate buffer (pH 7.4) and 5.0 mM $[Fe(CN)_6]^{3-/4-}$, after incubation in the different concentrations of cDNA. (d) The calibration curve of ΔR_{ct} versus logarithm of cDNA concentration.

The specificity of the pDNA/AuNPs-PAT/rGO/GC genosensor towards different target DNA sequences including complementary, non-complementary two-base, three-base mismatched was investigated using DPV technique and their voltammograms are presented in Fig. 6. It is obvious that after incubation of the genosensor with complementary target (cDNA) there was a marked decrease in peak intensity revealing the process of hybridization. Incubation of non-complementary and three-base mismatched showed no significant change in the voltammogram of pDNA/AuNPs-PAT/rGO/GCE, suggesting that no hybridization is taking place.

While, incubated of two bases mismatched on the pDNA/AuNPs-PAT/rGO/GCE, there was a light decrease in peak current in contrast with that of the pDNA. This might be because of the partial hybridization of pDNA. These outcomes uncover the selectivity and specificity of the proposed genosensor towards different target DNA sequences.

3.5. Real sample analysis

Serum samples were collected from normal persons, and stored frozen until assay. 2 mL of methanol was added to 1.5 mL of serum. After vortexing of the serum samples for 5 min, the precipitated proteins were separated by centrifugation for 10 min at 14000 rpm and filtrated through a 0.45-μm milli-pore filter. Finally, the treated serum samples were diluted to 10 mL with PBS (0.1 M, pH = 7.4). Afterward, the desired amount of cDNA was spiked to the serum samples to deliver the mentioned concentration shown in Table 1. The standard addition method was employed to record analytical signals via EIS. The accuracy of the used procedure was evaluated by calculating the recoveries of the cDNA in the real samples that varied from 91.4% to 104.0%. The precision of the proposed method was evaluated using calculating the relative standard deviations ranged from 4.2% to 5.8%. The results reveal the acceptable application of the extended genosensor for the assay of the β-thalassemia gene in human's serum samples.

4. Conclusion

We have presented an efficient DNA electrochemical genosensor for over-sensitive detecting β-thalassemia gene. We produced the DNA biosensor using immobilizing thiol tagged probe DNA on AuNPs-PAT modified rGO/GCE. AuNPs-PAT/rGO shows a large surface area for immobilizing probe DNA. $[Fe(CN)_6]^{3-/4-}$ was selected as a proper electrochemical probe for the “signal off” (DPV) and “signal on” (EIS) approaches. The proposed biosensor is greatly selective, sensitive and remains significantly activity (86% of the initial activity) following 15 days of use at the ambient temperature. Therefore, the biosensor developed in this study could be a critical device for specifying the existence of low concentrations of β-thalassemia gene. This genosensor is the second work in specific detection of thalassemia gene.

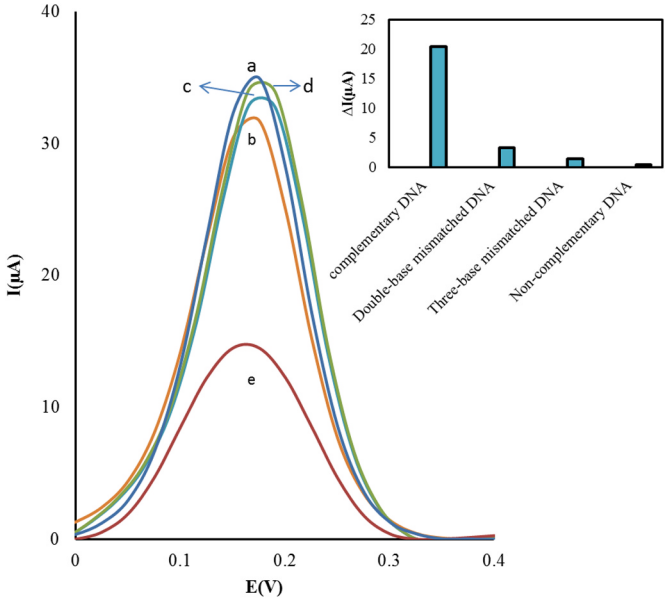

Fig. 6. DPV signal: (a) pDNA/AuNPs-PAT/rGO/GCE, (b) pDNA/AuNPs-PAT/rGO/GCE hybridized with two base mismatch sequences, (c) pDNA/AuNPs-PAT/rGO/GCE hybridized with three base mismatch sequences, (d) pDNA/AuNPs-PAT/rGO/GCE hybridized with non-complementary sequences and (e) pDNA/AuNPs-PAT/rGO/GCE hybridized with complementary sequences (20 pM of each compound).

Table 1
Results of the recovery analysis of cDNA spiked serum samples (n = 3).

No.	cDNA added (M)	cDNA found (M)	Recovery %	RSD%
1	1.0×10^{-12}	9.14×10^{-13}	91.4	4.2
2	1.0×10^{-11}	9.42×10^{-12}	94.2	5.8
3	1.0×10^{-10}	1.04×10^{-10}	104.0	5.1

Acknowledgments

The authors gratefully acknowledge the support of this work (with grant number 57021) by the Research center of Razi University, Iran, 97/303200 for financial support.

Appendix A. Supporting information

Supplementary data associated with this article can be found in the online version at doi:10.1016/j.bios.2019.01.017.

References

Cai, B., Wang, S., Huang, L., Ning, Y., Zhang, Z., Zhang, G.J., 2014. ACS Nano 8, 2632–2638.
Chen, D., Feng, H., Li, J., 2012. Chem. Rev. 112, 6027–6053.
Chen, L., Tang, Y., Wang, K., Liu, C., Luo, S., 2011. Electrochem. Commun. 13, 133–137.
da Silva, J.V., Madurro João, A.G.B., Madurro, J.M., 2017. J. Solid State Chem. 21, 2129–2139.
Dolatabadi, J.E.N., Mashinchian, O., Ayoubi, B., Jamali, A.A., Mobed, A., Losic, D., Omidi, Y., Guardia, M., 2011. Trends Anal. Chem. 30, 459–472.
Frias, I.A.M., Andrade, C.A.S., Balbino, V.Q., de Melo, C.P., 2017. Carbon 117, 33–40.
Hamidi-Asl, E., Raoof, J.B., Naghizadeh, N., Akhavan-Niaki, H., Ojani, R., Banihashemi, A., 2016. Int. J. Biol. Macromol. 91, 400–408.
Jaiswal, N., Pandey, C.M., Soni, A., Tiwari, I., Rosillo-Lopez, M., Salzmann, C.G., Malhotra, B.D., Sumana, G., 2018. Sens. Actuators B Chem. 275, 312–321.
Jiang, W., Wu, L., Duan, J., Yin, H., Ai, S., 2018. Biosens. Bioelectron. 99, 660–666.
Kashish, Gupta, S., Dubey, S.K., Prakash, R., 2015. Anal. Methods 7, 2616–2622.
Liu, X., Li, Y., Zheng, J., Zhanga, J., Sheng, Q., 2010. Talanta 81, 1619–1624.
Low, S.S., Loh, H.S., Boey, J.S., Khiew, P.S., Chiu, W.S., Tan, M.T.T., 2017. Biosens. Bioelectron. 94, 365–373.
Lu, C.H., Yang, H.H., Zhu, C.L., Chen, X., Chen, G.N., 2009. Angew. Chem. 121, 4879–4881.
Lucarelli, F., Tombelli, S., Minunni, M., Marrazza, G., Mascini, M., 2008. Anal. Chim. Acta 609, 139–159.
Mohammadian, N., Faridbod, F., 2018. Sens. Actuators B Chem. 275, 432–438.
Moon, J.M., Thapliyal, N., Hussain, K.K., Goyal, R.N., Shim, Y.B., 2018. Biosens. Bioelectron. 102, 540–552.
Oliveira, D.A., Silva, J.V., Flauzino, J.M.R., Castro, A.C.H., Moço, A.C.R., Soares, M.M.C.N., Madurro, J.M., Brito-Madurro, A.G., 2018. Anal. Biochem. 549, 157–163.
Sadik, O.A., Aluoch, A.O., Zhou, A., 2009. Biosens. Bioelectron. 24, 2749–2765.
Scarano, S., Mascini, M., Turner, A.P.F., Minunni, M., 2010. Biosens. Bioelectron. 25, 957–966.
Shamsipur, M., Farzin, L., Amouzadeh Tabrizi, M., Shanehsaz, M., 2016. Mater. Sci. Eng. C 69, 1354–1360.
Sharma, S., Sharma, S., Singh, N., Tomar, V., Chandra, R., 2018. Biosens. Bioelectron. 107, 76–93.
Shi, A., Wang, J., Han, X., Fang, X., Zhang, Y., 2014. Sens. Actuators B Chem. 200, 206–212.
Shin, H.S., Huh, S., 2012. ACS Appl. Mater. Interfaces 4, 6324–6331.
Tiwari, I., Singh, M., Pandeya, C.M., Sumana, G., 2015. Dalton Trans. 44, 15557–15566.
Wang, W., Wang, W., Davis, J.J., Luo, X., 2015. Microchim. Acta 182, 1123–1129.
Wilson, J., Radhakrishnan, S., Sumathi, C., Dharuman, V., 2012. Sens. Actuators B Chem. 171–172, 216–222.
Zare, Y., Shabani, I., 2016. Mater. Sci. Eng. C 60, 195–203.
Zhao, H., Jia, X., Wang, B., Wang, N., Li, X., Ni, R., Ren, J., 2015. Biosens. Bioelectron. 65, 23–30.
Zhou, M., Zhai, Y., Dong, S., 2009. Anal. Chem. 81, 5603–5613.